

Visualization and analysis of medical ultrasound processing applied to Ground Penetrating Radar

Ground Penetrating Radar (GPR) is used in asset management to survey the state of buried pipelines, but analysis of the resulting radargrams can be difficult, subjective and time consuming. Thomas Deserno, Karsten Müller, Markus Reiss, Gael Pentang, Daniela Hofmann and Jürgen Niessen in this paper discuss the application of medical ultrasound processing techniques to GPR data in order to make the evaluation of radargrams faster and more accurate.

Ground Penetrating Radar (GPR) is a technique for non-destructive detection and illustration of buried objects and cavities as well as soil layers and water table. GPR is based on actively emitting electromagnetic waves in a medium, usually in form of impulses. Along its path, the radar signal is scattered, reflected and diffracted at discontinuities, as well as attenuated through absorption. The running time of the signal is a measure for the spatial depth of objects. The reflection data is registered and edited to form a so-called radargram.

The major problem facing the GPR technique is the difficulty associated with the visualization and interpretation of the radargrams. Currently, this is still done manually and, therefore, is subjective and time consuming. Available software packages support only basic manipulation of the image data, which includes background removal, noise filters, and edge enhancement. The interpretation of a radargram is difficult and requires an expert's experience (see Figure 1). Therefore, improving the processing of GPR data is still a major field of research. Contrarily, medical three-dimensional (3D) ultrasound is likewise based on reflection signals, but automated analysis, visualization, segmentation and interpretation of such data has already been well established. Figure 2 exemplifies the developments that have been achieved in medical applications.

In this paper, we aim at interfacing GPR data to medical ultrasound and applying medical image visualization and processing techniques to GPR data for improved asset management (Figure 3). This paper introduces a converter software that aims to interface medical ultrasound with GPR data, allowing the application of

medical image visualization and processing techniques to GPR data. From the GPR radargrams stored in DZT format, corresponding ultrasound files conformant with the Digital Imaging and Communications in Medicine (DICOM) standard are generated and rendered into volumes with ImageJ and the Medical Imaging and Interaction Toolkit (MITK).

As a result, hybrid visualization is obtained where direct volume rendering is combined with model-based surface reconstruction of cylindrical pipes, pipe systems, cavities, and other basic structures. Furthermore, the interface allows the application of medical image processing and analysis to GPR data.

Ground Penetrating Radar (GPR)

GPR is based on actively emitting electromagnetic waves in a medium, mostly in the form of impulses with dominant frequencies in the range of approximately 20 MHz to 2 GHz. The frequencies used for investigating the subsoil are between 400 and 1000 MHz.

Along its path, the radar signal is scattered, reflected and diffracted at discontinuities, as well as attenuated through absorption. The dielectricity constant $\epsilon = \epsilon_0 \cdot \epsilon_r$ is the relevant physical magnitude. Since ground material components are not uniform, ϵ_r is continuously subject to fluctuations. Decisive for a reflection is a transition from one medium with a low ϵ_r into one with a high ϵ_r or vice-versa. As a result, the dielectric conditions in the ground are imaged. During the propagation in the medium, the signal experiences a material-dependent attenuation. The higher the conductivity σ , the lower the penetration depth. Since conductivity is dependent upon frequency, the penetration is depth attainable. The running time of the signal is a measure for the positional

Thomas M Deserno, RWTH Aachen University, Department of Medical Informatics, Aachen, Germany. Email: deserno@ieee.org

Karsten Müller, RWTH Aachen University, Research Institute for Water and Waste Management, Aachen, Germany. Email: mueller@fiw.rwth-aachen.de

Markus Reiss, RWTH Aachen University, Research Institute for Water and Waste Management, Aachen, Germany. Email: reiss@fiw.rwth-aachen.de

Gael Pentang, RWTH Aachen University, Department of Medical Informatics, Aachen, Germany. Email: gpentang@mi.rwth-aachen.de

Daniela Hofmann, GBM Wiebe – Gleisbaumaschinen GmbH, Achim, Germany. Email: dhofmann@wiebe.de

Jürgen Niessen, GBM Wiebe – Gleisbaumaschinen GmbH, Achim, Germany. Email: jniessen@wiebe.de

© IWA Publishing 2010

depth of objects [1]. The reflection data is registered and edited to form a radargram (Figure 4) [2].

The soil consists of different materials, which form a layer of different dielectricity. Radar waves emitting from the transmitter are partly transmitted and reflected, and from the runtime of the signal, spatial position is computed. Foundations, pipes, water, and other embossed structures result in full reflection, which is clearly observed in the radargram by its sinusoid pattern.

Objects in the underground can be detected with this method regardless of their material, provided that the contrast of dielectrical constants of the discovered structure and the surrounding material is sufficiently high. The lateral position of any object can be determined, usually with the help of radargrams, with an accuracy of 10cm. The error in depth determination is within 5% to 10% [2]. Considering a mostly homogeneous soil, anomalies of existing cavities or dispersions in the soil can be derived directly from the results of GPR measurements [4].

Because GPR data interpretation needs co-location with external

information like geologic data, geo-referencing has been established [5]. Using a GPS (Global Positioning System) (Figure 5) GPR data is arranged in a geospatial coordinate system.

The result of geo-referencing is visualized in Figure 6. From a large field, several scans have been obtained, which may partly overlap and usually incompletely represent the areal. Using Georail-Sprinter, each scan is composed of 14 measurements per row. After geo-referencing, the individual scans can be combined to represent a larger volume of ground surface.

Visualization of GPR data

Currently, a small number of visualization techniques are available to display GPR data. In the following, these techniques are briefly reviewed.

2D standard data visualization

The easiest way of showing a radargram to the inspector is directly displaying the raw data. Each scan of each antenna is shown individually, and pseudo-colouring is usually applied to support manual interpretation and analysis. In addition, artifacts and noise may be removed automatically or semi-automatically by digital filtering of the raw data. In the radargram, suspicious signatures manually are



marked and commented by the user. For example, Figure 7 shows a radargram with three manual annotations indicating soil infiltration of water from a crossing pipe, loose soil, and a crossing line without any finding for annotations A, B, and C, respectively.

3D geo-referenced data visualization

The individual scans of each antenna array can be combined using the geo-references from the GPS signal. A 3D radargram is formed, and usually displayed again using pseudo-colouring. The 3D visualization software supports browsing individual slices, and – beside filtering and noise removal – thresholding can be applied to extract structures of high signal amplitude (Figure 8).

Despite its high resolution and that the complex 3D information is visualized at a glance, this display option has disadvantages as well. Only



Figure 1
Left: Investigation of embankment with GPR. Right: Resulting radargrams with cavity signatures from muskrats highlighted.

the information won by the radargram data is shown, however an evaluation of the signatures on the radargram is difficult. For instance, an evaluation of a radargram from an investigation of three conduits where metal plats, breakdown bodies and tanks filled with air and water were inserted, does not give precise information about the structures. Manly because volume rendering techniques, as used in the medical area, have not yet been included.

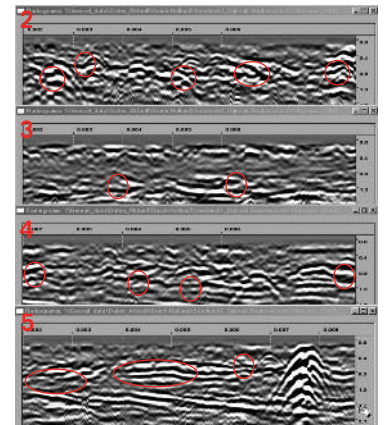
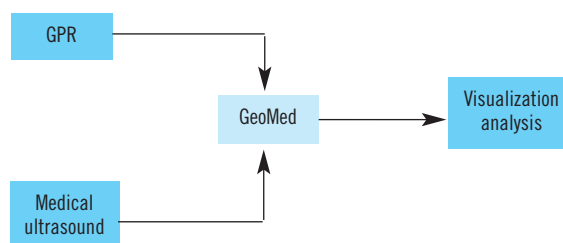
2D geo-referenced model visuals

Visualization of models rather than raw or pre-processed radar data has also been suggested [5]. In contrast to 3D geo-referenced visualization, the GPR information is now used for co-location of structures into existing plans. In this way, an overview is quickly provided to the inspector using a well-known representational form (Figure 9).

Technically, the radargram data is transferred into a 2D geo-referenced representation and symbols, which are related to different structures of interest manually located in the radargram, and are overlaid or merged into existing plans. In Figure 9, for instance, circular objects are displayed to visualize suspicious structures from the GPR signal. This type of visualization is based on geographic information systems (GIS) and tools for computer-aided design (CAD) [6]. However, this feature of 2D models is also their drawback. For many applications, model visualization might be too abstract, because the information displayed no longer corresponds to the signal measured, since too many details are disregarded. In particular, the sinusoid reflection patterns are lost.

Figure 2
Medical ultrasound. A 3D surface extraction allows applying rendering techniques

Figure 3
The GeoMed project aims at merging GPR data with medical ultrasound techniques for improved visualization and data analysis



Medical 3D data visualization and processing

A couple of commercial systems for developing medical image processing and visualization exist. However, we focus on packages in the public domain since these frameworks usually allow user specific extensions and adaption.

ImageJ

ImageJ is a Java-based image processing programme developed by Wayne Rasband at the National Institute of Mental Health (NIH) in the US [7]. It was designed with an open architecture that provides extensibility via a lot of powerful Java plug-ins and recordable macros. It is therefore completely platform independent and runs under Windows, Linux and MacOS [8]. Custom acquisition, analysis and processing plug-ins can be developed using ImageJ's built-in editor and a Java compiler. Together with user-written plug-ins, ImageJ makes it possible to solve standard and specific image processing and analysis problems, particularly in the medical domain. It can display, edit, analyse, process, save and print any common 8-bit, 16-bit and 32-bit image format, including digital imaging and communication in medicine (DICOM) files and raw data, as well as series of images. The latest version of ImageJ updates documentation test images and a growing collection of provided plug-ins can be downloaded from the ImageJ homepage [9]. The complete software source code is available online and details about its simple installation can be found in the ImageJ tutorial at the ImageJ homepage.

The programme can import 'stacks', e.g. a series of DICOM images of the same size and type in a folder, and display them in the same window [9]. The loaded stack can be rendered in a volume with the volume viewer plug-in. The object is displayed in a side window in three different views. Depending on the chosen view, a section plane can be selected and modified by shifting the object in the

main window. The resulting representation can be rotated in all three dimensions and each layer can be shown according to the alignment of the sectional planes.

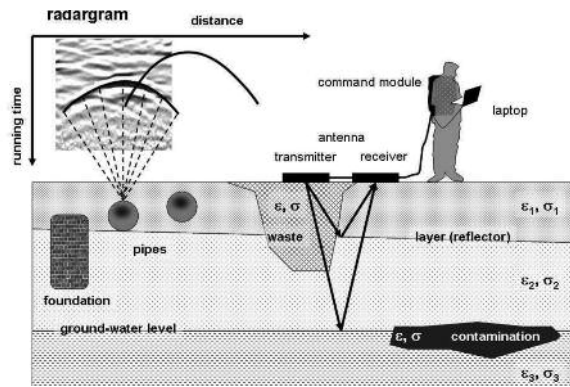
MITK

The Medical Imaging Interaction Toolkit (MITK) is a free C++ open source software system for development of interactive medical image processing software that can handle non-medical data as well [10]. It was originally developed as a common framework in the Division of Medical and Biological Informatics (MBI) at the German Cancer Research Centre (DKFZ).

MITK is a class library based on and extending the Insight Toolkit (ITK), that forms the algorithmic basis for data registration, interpolation and segmentation, and the Visualization Toolkit (VTK), providing powerful visualization capabilities. So, the main purposes of MITK are to reduce the effort required to construct specifically tailored, interactive applications for medical image analysis (segmentation, registration) and supporting easy combination of algorithms, which have been developed by ITK, with visualizations that have been created by VTK for the development of interactive medical imaging software [11, 12]. MITK is able to process different 2D and 3D data. Among these are DICOM files, point sets, sets of 2D slices, and surface files.

Re-using the design principles of ITK and VTK, MITK is an object-oriented, cross-platform library with classes that are derived from top level classes of ITK. It uses a data-centred approach in which the central elements representing the model are data objects and data trees. A data object represents and provides access to data. It can be created and updated by process objects connected together to a data processing pipeline. A data tree allows hierarchical organisation of multiple data objects. Objects within the data tree are created and updated by process objects. A pipeline may be constructed, automatically affecting all references to the constituents of the pipelines. Optionally, properties like colour, opacity, visibility, etc. can be added to data objects. These properties apply to all views of the data, rendered into different windows, by default, but may be changed for each view if required. For example, a data object may be visible in all but one view.

In particular, MITK allows joint visualization of 3D data, which is directly rendered, and data segments as well as artificial models, which are represented by their triangulated surface. Figure 10 exemplifies this type



of combined visualization. Maximum intensity projection is used for volume rendering, and the orbital areas are displayed using surface rendering.

GPR imaging and data handling

All measurements were done using the 'Georail Sprinter' device by GBM Wiebe Ltd. (see Figure 5), which is based on a TerraVision array of 14 bi-static 400 MHz turnstile dipole antennas (see Figure 6). They are installed in parallel on a trailer with a distance to the surface of 2-3cm. Due to the arrangement of the antennas, it is possible to detect objects like pipes in the ground. The array is about 2.2 m wide, so that a lane can be ascertained entirely at a single pass. GPS recording and geo-referencing of the radargrams is performed.

The database contained a total of 117 GPR files recorded in the German cities of Cologne, Detmold, Nuremberg, Otzenrath and Rosslau. These files resulted from road as well as from embankment inspection. Typical image resolutions are 14 x 512 x L, where L denotes the length of the measured section. In our data, $L_{min} = 503$ and $L_{max} = 17,831$.

All data is stored in DZT format containing all the 14 measurement profiles (so called passes). The DZT file format corresponds to the Radan format for geophysical survey system interface (GSSI). GSSI files have either a 512-byte (old style) or 1024-byte (current style) header [13], sequentially followed by the proper image data (Figure 11).

The header gives information about the data type used to code the image,

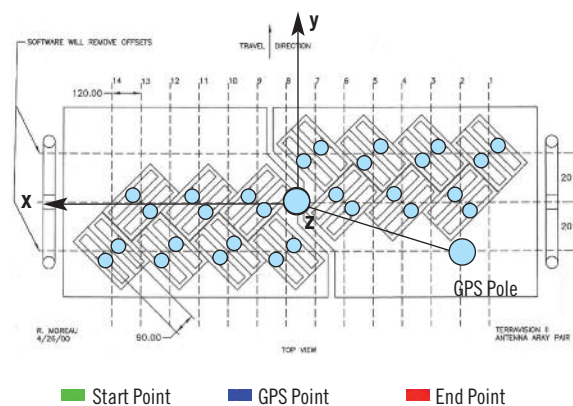


Figure 4 Measuring principle of GPR data [3]

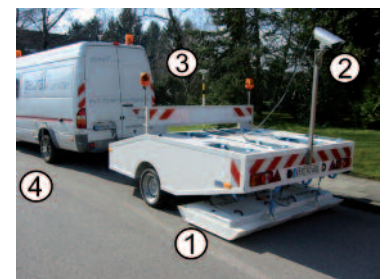
Figure 5 GPR Imaging Device (Georail Sprinter). The vehicle for road analysis consists of (1) an array of 14 radar antennas, (2) optical camera, (3) GPS module, and (4) distance measurement unit

the image identification, an offset that indicates where the pass data begins and the dimensions of each pass. In addition, important metadata on system characteristics, as well as GPS coordinates, can also be found in the header of the georadar file (Figure 12).

DICOM standard in medical imaging

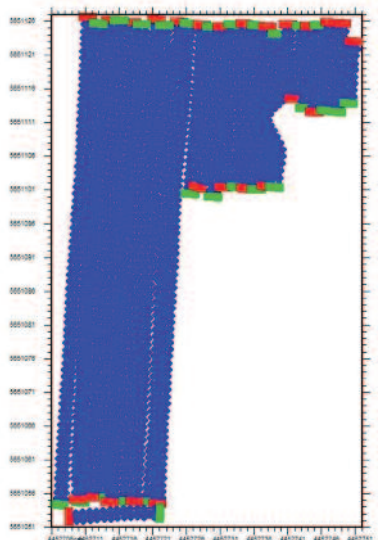
DICOM is a common standard for exchanging medical image data and diagnostic information between image acquisition systems, such as x-ray, ultrasound, computed tomography (CT), magnetic resonance imaging (MRI), viewing stations, and the archive to form picture archiving and communication systems (PACS). For these purposes, DICOM defines:

- Objects such as images and all kind of meta data including patient, study,



- and pathology data,
- Syntax and semantic of commands needed for information transmission, and
- The protocols for transmission.

The DICOM standard is based on a tag value representation. A tag uniquely labels an information element. The basic element (tag, value representation, value length, and value field) is called attribute. Many attributes form an information object. An information object is an abstraction of a real world entity (e.g., a CT image, a study, etc.) which is acted upon by one or more service classes and is member of



an information object class with a particular information object definition (IOD). A service class represents a structured description of services which are supported by cooperating DICOM application entities acting on a specific class of information objects. An important element within the DICOM object model is the service object pair (SOP) which combines an information object with an applicable service class (Figure 13). This is the fundamental unit, which allows interoperability with the DICOM standard.

A single DICOM file consists of an introductory header followed by a stream of DICOM object (Figure 14). The DICOM header includes a 128-byte preamble and a 4-byte prefix 'DICM' directly followed by metafile information [14]. By this nature, DICOM is easily extensible, and can be adapted to future modalities that may be introduced in clinical use. In this case, several information objects may be re-used and referring to the attributes and the data dictionary defining almost 30 value representations, application specific information can be modelled, too [15]. However, to ensure interoperability, we are not aiming at defining new GPR information objects but use existing ultrasound objects to host the relevant meta information (see Figure 12).

Data conversion

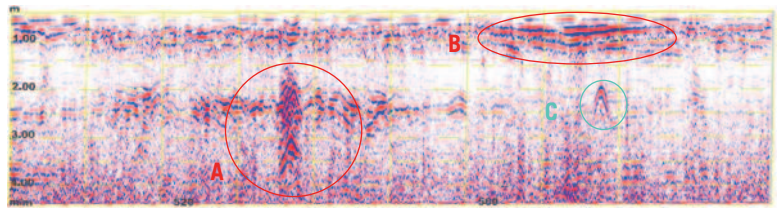
Data conversion is not implemented from scratch but refers to existing toolboxes. In particular, we use the DICOM toolkit and DICOM3Tools, which are briefly introduced before our conversion algorithm is presented.

The DICOM toolkit (DCMTK) was developed at the Research and Development Institute for Information Technology Tools and Systems in Oldenburg [16]. It implements a large part of the DICOM standard in C++ programming language. The toolkit is platform-independent and a variety of libraries and resulting programmes are freely available. It is continuously developed according to the DICOM standard and is used both for testing and commercial development.

The official version of DCMTK includes modules for standard library functions (ofstd), network communication (dcmnet), worklist management (dcmwlm), images (dcmimage), JPEG compression (dcmjpeg), digital signatures (dcmsignl), data sets and files (dcmdata), simple image archives (dcmqrdb), image data (dcmimgle), presentation states (dcmpstat), secured transfer (dcmfsl), and structured reporting (dcmsr).

The dcmdata module offers for

Figure 7
2D standard data visualization (pseudo-coloured radargram with manual annotations)



example a class library for reading, processing and storing of DICOM files. These functions can read and write DICOM files in different transfer

included in the Dicom3Tools is used to convert RAW files into DICOM files. It requires as input parameters the RAW data, its height and width, the number of bits per pixel, the number of samples, and the photometric interpretation to generate the corresponding file in DICOM format.

Based on these tools, a script was developed that converts a 2D georadar file with several passes into a series of DICOM images. The script is based on a predefined folder structure in which the source files are stored together with an empty log file in a folder and the resulting DICOM files are written in another folder. These folders can be specified by the user as input parameters at script execution. The necessary input parameters are:

- The georadar file to be converted,
- The input folder for temporary files, and
- The output folder for storage of the resulting DICOM files.

syntaxes and are relatively error-tolerant for false coded files. Additionally, a complete electronic DICOM data dictionary is available. Practical example applications include displaying a DICOM file in textual form on the console with dcmdump and creating a DICOMDIR index file for DICOM disc with dcmgmdir. DCMTK also contains the dcmofid function used in the programme to insert, modify and delete individual DICOM attributes. This function is globally installed and can be accessed from the command line with the corresponding parameters (day, optional: value, path to the DICOM file).

The Dicom3Tools of David Clunie is an extension of the DCMTK package with practical examples and new functionalities. The rawtode function

After setting and exporting the PATH- and the DCMDICTPATH-environment variables conveniently, the DICOM dictionary can be loaded to execute the script for file conversion. The conversion process includes the decomposition of the georadar scan into individual PNG slices, and the header information is stored in a log file. Then, a standard LINUX function is used to generate corresponding RAW files from the PNG format. The conversion of image files from RAW format to DICOM format is done with a predefined method of the DICOM toolkit. Finally, the dcmofid function of the Dicom3Tools is used to configure the obtained DICOM files into 2D DICOM conform ultrasound images. All the attributes with the tag group number '0002' are determined by the DCMTK and their values are assigned so that subsequent modification of these attributes is not possible. All other attributes can be modified manually to change their default values. Some examples on the information transfer table are given below:

- The image type is constant and has the predefined value 'DERIVED PRIMARY' since the DICOM series results from the conversion of a georadar file. In this context, constant means that this attribute has the same value for all the converted

Figure 8
3D geo-referenced data visualization

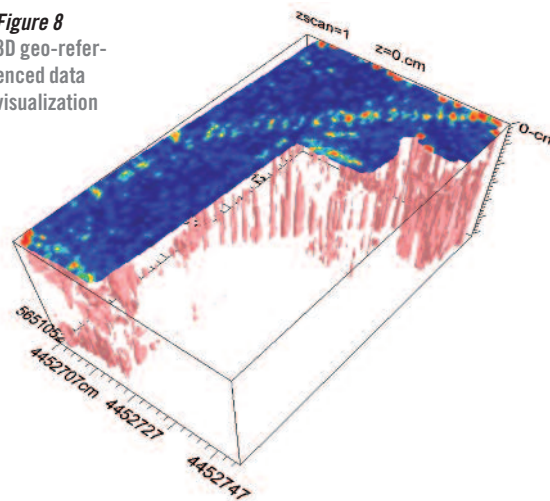


Figure 9: A 2D geo-referenced model visualization. It shows a top-down view of a site plan with a sewer line and GPR objects. A blue line represents the sewer, and green circles represent GPR objects. Labels include 'section of sewer' and 'GPR objects'. A scale bar at the bottom right indicates 0-20m.

Figure 9
2D geo-referenced model visualization [6]

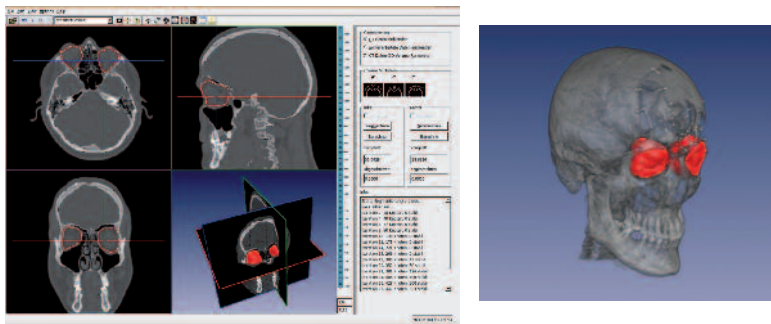


Figure 10
Medical volume data visualization. Left: The MITK application has four coupled viewing windows for axial, sagittal, coronar and combined view, where the corresponding reticles are shown. Right: The fourth viewing window may also be used to display joint volume / surface renderings.

georadar files of this study. It should be noted that this value should be specified explicitly by the user.

- The attributes 'instance creation time' and 'instance creation date' are automatically set by the script to the current date and time of the DICOM file creation.
- The SOP Class UID and the SOP Instance UID are set from the toolkit.
- The values for the attributes 'study date' and 'time study' are taken from the variables rhb_cdt of the georadar file (see Figure 12). These values vary

- The value of the DICOM attribute 'patient's sex' is constant and set to 0.
- The image number is set from a counter variable that is incremented during image formation. In georadar files, no indication of the number of samples per pixel is given, so it is automatically assigned to the default value of 1 and is not modified.
- The photometric interpretation is set constantly to the value of 'MONOCHROME 2' because the

header	pass 1	pass 2	...	pass n
--------	--------	--------	-----	--------

rh_tag	tag	2047	rh_nchan	number_of_channels	1
rh_data	1024	1024	rhf_epsr	average_dielectric_constant	5,0
rh_nsamp	samples_per_scan	512	rhf_top	position_in_m	0.368951
rh_bits	bits_per_data_word	16	rhf_depth	range_in_m	3,000
rh_zero	offset	0	rh_coordX	x_coordinates	0,000 27.150
rhf_sps	scans_per_second	105,000000	rhf_servo	levelservo_level	0,000
rhf_spm	scans_per_meter	40,000000	rh_accomp	ant_conf_component	0
rhf_mpm	marks_per_meter	0,333333	rh_sconfig	setup_config_number	0
rhf_position	position_ns	5,500000	rh_spp	scans_per_pass	1087
rhf_range	range_ns	44,721359	rh_linenum	line_number	0
rh_npass	number_of_passes	14	rh_coordY	y_coordinates	0,000 1,560
rhb_cdt	creation_date	13.03.2007 11:00:00	rh_lineorder	line_order	8
rhb_mdt	modification_date	13.03.2007 11:00:00	rh_sliceType	4:slice_type	0
			rh_dtype	dtype	0
			rh_antname	antenna_name	TERRAVISION2

Figure 11
DZT file format structure

Figure 12
Exerpt of metadata in DZT header

- for different files.
- The modality is set manually to ultrasound for ultrasound imaging. This value is constant for all the DICOM series generated in scope of this work.
- The conversion type WSD is set automatically. It describes the type of image conversion for generating a DICOM file. In this case, a workstation is used. The values of manufacturer of the computer for data collection as well as the company doing the data generation are constant and should be modified manually.
- Referenced SOP Class UID and SOP Instance UID Referenced generate a connection of the individual images of a series of pictures with each other. These referenced images have the same SOP Class UID as that of the current image. The referenced SOP Instance UID is the same.
- The name of the image series is taken from the GPR tag rh_name and stored in the DICOM attribute patient name.
- The value of the DICOM attribute patientID is composed from the study time and study date and is automatically set by the script.

- The data only contains gray values. By default, the number of frame is set to 1, but this is modified according to the variable rh_npass and set constant to 14.
- The values of the DICOM attribute rows and columns are respectively taken from the variables rh_nsamp and rh_spp. These values vary depending on the GPR data.
- The pixel spacing cannot be deduced from the GPR data. Therefore, it is set constantly to a ration of one.
- The value of the attributes bits allocated, bits stored and high bit result from the photometric interpretation. This data also is constant. The data format manually based on the pixel representation is set to an unsigned Int type 000H.
- Since the images undergo a compression during the processing, the attribute 'lossy compression' takes the value 01.

After setting all these DICOM attributes, the conversion in a 2D DICOM ultrasound series is performed and GPR data can be read, displayed and further processed by any medical software compliant with the DICOM standard.

Models to visualize

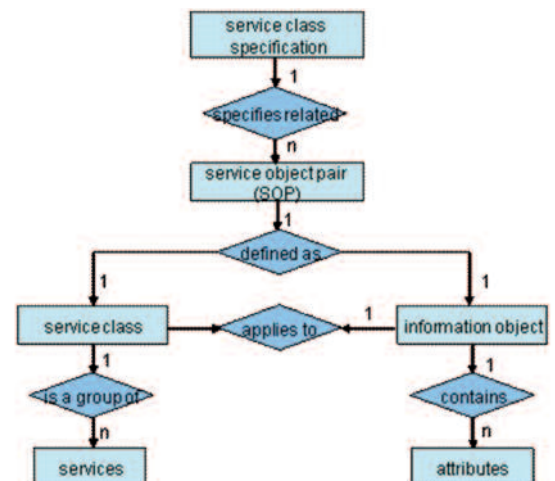
However, we do not only aim at visualizing the GPR signal, but use medical software and programmes for hybrid data and model visualization. As it is commonly accepted in the medical field, such visualization essentially can simplify the understanding of complex image data such as ultrasound and GPR.

GPR surveys are now commonplace in environmental and engineering geophysics for non-destructive investigation of the shallow subsurface. Underground infrastructures that need to be investigated are channels, sewers, pipes, as well as special structures, but also cavities that are present on defect pipes. The investigation of cavities is also interesting for embankment inspection since it can help to detect damages of the sandy underground construction that might become crucial on floodwater conditions. In terms of abstract visualization models, GPR data portions of sewers and drainage systems can be simply visualized by a series of geometric objects (Table 1).

Results

The primary goal when processing GPR data is to detect relevant information for interpretation and analysis to support appropriate asset management. Using the developed converter software, GPR data can be transformed into a series of medical ultrasound images for DICOM compliant volume visualization. Currently, the header of GPR data is composed of more than 40 parameters that are used to encode the radar signals. These parameters include the number of channels, distance of antennas, creation date and time, GPS information and other electrical parameters. They are mapped to DICOM image object definitions. Basically, image modules such as 'general image', 'image pixel', 'device', 'US region calibration', 'US image',

Figure 13
Entity relationship model of DICOM elements



and 'palette color lookup table' are used to embed the relevant tags.

As result, direct volume rendering of GPR is possible. Figure 15 shows an example of GPR data visualized as medical ultrasound in ImageJ. The volume illustrates a GPR measurement carried out on a portion of road. A suspicious area that shows a cavity can be seen. A relevant structure is also marked on the picture.

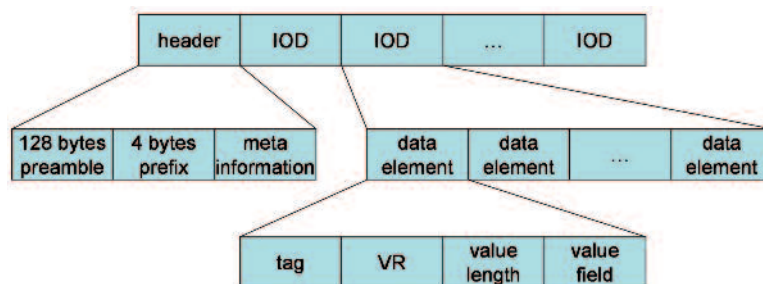
Hybrid visualization of volume data and abstract models is supported using the MITK toolkit. Figure 16 shows the same data as displayed in Figure 15. MITK, however, additionally allows user-guided exploration of 3D data, segmentation and visualization of hierarchically organized surface models and volume data [17]. Therefore, MITK is suitable to combine GPR data volume rendering with model-based surface reconstruction of models representing the relevant structure (pipe) and the suspicious region (cuboid). Figure 17 presents different views of hybrid visualization.

In summary, medical image processing and visualization becomes available for GPR data. Direct volume rendering techniques with the ImageJ software as well as combined volume surface visualization modes with MIT allow simplified analysis and interpretation of GPR radargrams after conversion into the DICOM US format.

Discussion and conclusion

In this paper, our goal was to prove the concept that image visualization, processing and recognition algorithms developed and tested for medical ultrasound are adaptable to GPR data and make the evaluation of radargrams faster and more accurate.

Figure 14
The DICOM image file structure



In particular, the illustration of GPR data with precious visualization programmes is extensive and offers frequently just the data representation, and interpretation still is difficult for communal decision makers. To obtain a better visualization, GPR data was transformed in DICOM format, which is already established in the medicine sector. Thus, the illustration of GPR data is possible by means of medicine image processing programmes. To relieve the interpretation of radargrams, it has been analysed, if the algorithms, which are already used for medicine ultrasound, are adapted for GPR information. The visualization of buried objects and soil layers can be enabled with simple symbols and their combinations in 3D presentations. In medical research, these techniques are used already successfully. For illustration of subterranean infrastructure and layers, however, it still has to be tested.

To acquire GPR data, it is reasonable in the first step to operate in a less complex environment (for instance a levee). There are less disturbing objects like unknown fragments, boulders or layers, which complicate the identification of the located objects. In normal case, levees have exact interfaces (e.g. seal, gravel, compact soil), and if applic-

able a common sewer and cable system (e.g. drainage, pipes, cables). Thus, cavities can be identified more easily. In a following project, this basis shall be used to illustrate the internal structure of an embankment as a 3D model through using geo-referenced GPR data integrated into GIS by means of a bidirectional interface.

GPR is also applied to investigate complex environments. Here, the next step after illustrating a 3D model of the internal structure of an embankment is to picture the internal structure of a more complex environment. The identification and visualization of a subterranean infrastructure with complex cable and pipe systems, as well as unknown buried objects and constructions, will be enabled. ●

Acknowledgements

The project is supported by the excellence initiative of the German federal and state governments, RWTH pathfinder, ref OPEN25.

References

¹Gesellschaft für geophysikalische Untersuchungen mbH, *das Georadar, Karlsruhe (2003)*, available from: www.ggukarlsruhe.de (accessed 27 August 2009).
²Geo-Services GmbH (2004) *Das Georadar-*

Table 1
Idealized models for hybrid visualization

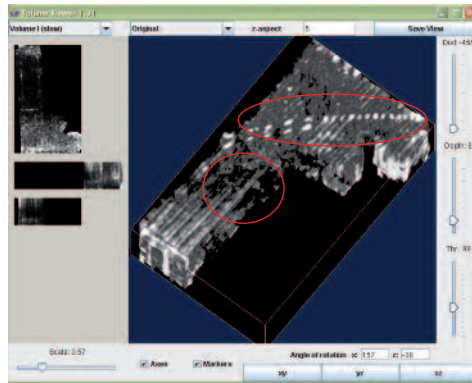
Buried objects and soil layers	Idealized illustration	Buried objects and soil layers	Idealized illustration
Pipe section		Cavities evolved from leaks in sewer e.g.	
Cavities, buried constructions of sewer		Soil layers, water table	
Sewer, drainage systems and cables		Cavities by means of muskrats (investigation of embankment systems)	
Sewer constructions, inspection points		Sewer in different soil layers	

Verfahren (Elektromagnetisches Reflexionsverfahren, EMR). Available from: www.geo-services.de/aktuell/oberflaeche-layout.htm (accessed 27 August 2009).

³Knödel K, Krummel H, and Lange G (1997) *Handbuch zur Erkundung des Untergrundes von Deponien und Altlasten, Band 3: Geophysik; Bundesanstalt für Geowissenschaften und Rohstoffe BGR, Springer-Verlag, Berlin, ISBN: 3-540-43683-9.*

⁴ATV-DVWK (2003) *ATV-DVWK M 150: Datenaustauschformat Teil 1: Zustandserfassung von Entwässerungssystemen. Hennef (Sieg):ATV-DVWK Deutsche Vereinigung für Wasserwirtschaft, Abwasser und Abfall eV, Hennef, Germany.*

⁵Stepkes H, Zimmermann J, Müller K, Siekmann M, and Pinnekamp J (2007)



Pinnekamp J, Müller K (2006). Influence of leaky sewers regarding stability of the surrounding ground and application possibilities of ground penetrating radars as a method for detecting and

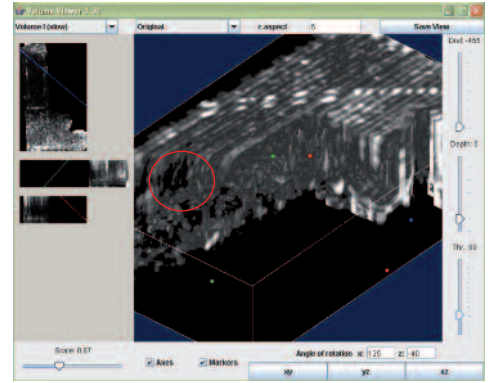


Figure 15 GPR data as used in Figure 8 is visualized in ImageJ. Left: Complete data set, the relevant structure and a suspicious cavity are marked. Right: Zoomed view of the suspicious cavity.

Department of Health and Human Services, United States, available from: www.nih.gov (accessed 31 August 2009)

⁸Burger W, Burge MJ (2006). *Digitale Bildverarbeitung, eine Einführung mit Java und ImageJ*, Springer-Verlag, ISBN 3-540-30940-3

⁹ImageJ, Image Processing and Analysis in Java, available from: <http://rsbweb.nih.gov/ij/> (accessed 31 August 2009).

¹⁰Bitter I, Van Uiter R, Wolf I, Ibáñez L and Kuhnigk JM (2007) Comparison of four freely available frameworks for image processing and visualization that use ITK. *IEEE transactions on visualization and computer graphics*, Vol. 13, No. 3, May / June 2007.

Figure 16 GPR data as used in Figure 8 is visualized in ImageJ

¹¹The Medical Imaging Interaction Toolkit (MITK), available from <http://www.mitk.org>, (accessed 31 August 2009)

¹²Wolf I, Vetter M, Wegner I, Nolden M, Böttger T, Hastenteufel M, Schöbinger M, Kunert T, and Meinzer HP (2004) The medical imaging interaction toolkit (MITK) – a toolkit facilitating the creation of interactive software by extending VTK and ITK. *Deutsches Krebsforschungszentrum (DKFZ), Division of medical and biological informatics, Im Neuenheimer Feld 280, D-69120 Heidelberg, Germany.*

Figure 17 Hybrid GPR data visualization is interactively explored using MITK

¹³Lucius JE and Powers MH (2002) *GPR Data Processing Computer Software for the PC: US Geological Survey Open-File Report 02-166*, 101p.

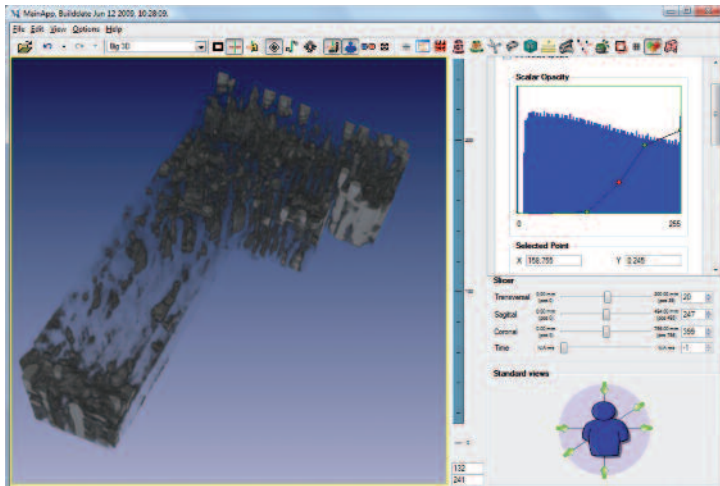
¹⁴National Electrical Manufacturers Association (NEMA) (2003). *Digital Imaging and Communications in Medicine (DICOM)*, available from <http://medical.nema.org>, Rosslyn, Virginia, USA (accessed 31 August 2009)

¹⁵Kuratorium: OFFIS, *Introduction to the DICOM standard*, available from <http://dicom.offis.de/dcmintro.php.en> (accessed 31 August 2009).

¹⁶OFFIS DCMTK Documentation, Oldenburg University and CERUM, 2005, available from <http://support.dcmtdk.org> (accessed 31 August 2009).

¹⁷Wolf I, Vetter M, Wegner I, Böttger T, Nolden M, Schöbinger M, Hastenteufel M, Kunert T and Meinzer HP (2005) *The Medical Imaging Interaction Toolkit. Med Image Anal; 9(6): 594-604.*

Paper presented at LESAM 2009 – 3rd IWA Leading-Edge Conference on Strategic Asset Management



Economic rehabilitation of sewer systems by ground penetration radar investigations. *Lesam 2007 – 2nd IWA Leading Edge Conference on Strategic Asset Management, Lisbon, Portugal.*

⁶Stepkes H, Hennerkes J, Zimmermann J,

assessment of bedding defects and cavities in the area of buried sewers. *Proceedings SOM 06 – 2nd International IWA Conference on Sewer Operation and Maintenance, Vienna, Austria*

⁷National Institutes of Health (NIH):

